




Microwave-assisted green synthesis of asphaltene-based carbon dots for micelle sensitized fluorescent probes

Meilin Liu¹, Xinyi Li¹, Yu Zheng¹, Yuhan Zhu¹, Taotao Li¹, Ziguo He¹, Cheng Zhang^{1,*}, and Kui Zhang^{1,*} 

¹ School of Chemistry and Chemical Engineering, Anhui Province Key Laboratory of Coal Clean Conversion and High Valued Utilization, Anhui University of Technology, Maanshan 243032, Anhui, China

Received: 2 September 2022

Accepted: 18 October 2022

Published online:

1 January 2023

© The Author(s), under exclusive licence to Springer Science+Business Media, LLC, part of Springer Nature 2022

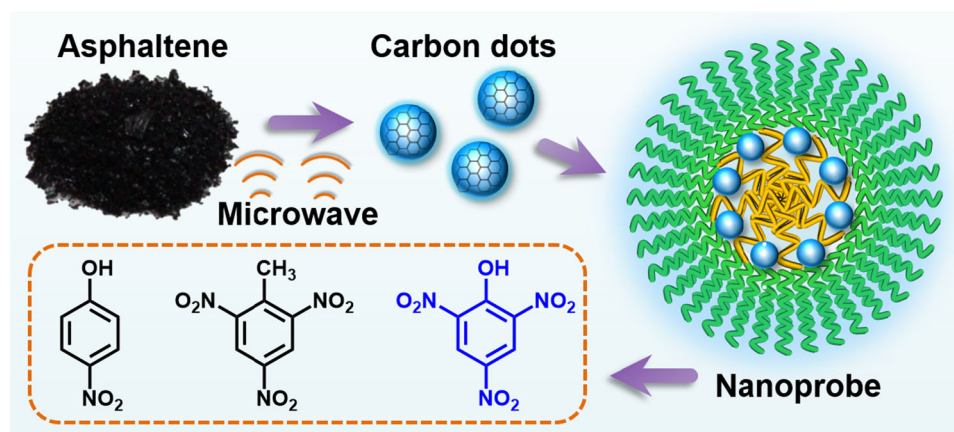
ABSTRACT

Development of inexpensive and environmentally friendly chemical sensors can help improve the global ecological environment and reduce pollutant emissions. In this work, asphaltene of coal liquefaction by-product was employed as the carbon source to fabricate carbon dots (CDs) by straightforward microwave radiation. The asphaltene-based CDs gave out blue emission under UV light excitation. Interestingly, the CDs are highly lipophilic because of its carbonized structure and insufficient hydrophilic groups. Based on these findings, an outstanding fluorescent sensor for 2,4,6-trinitrophenol (TNP) was developed by loading asphaltene-based CDs into polymeric micelles. The micelle formed by nonionic tri-block copolymers exhibited a hydrophobic inner cavity and hydrophilic surface. Due to the protection of the micelles, the emission of asphaltene-based CDs was enhanced by 2.89 times. But the fluorescence was significantly quenched by TNP through energy transfer and electron transfer mechanism, showing high sensitivity to TNP with a detection limit of 0.21 μM . The findings presented here provide a green method to synthesize fluorescent CDs and a promising strategy to design fluorescent probes.

Handling Editor: Annela M. Seddon.

Address correspondence to E-mail: czhang@ahut.edu.cn; zhangkui@mail.ustc.edu.cn

GRAPHICAL ABSTRACT



Introduction

Coal, a widely used fossil fuel, plays a significant role in power generation, metallurgical industry, and chemical manufacturing [1–3]. However, combustion of coal for electricity generation releases a large number of nitrogen oxides, sulfur oxides, carbon oxides, and solid particles into the atmosphere, leading to a serious environmental pollution [4, 5]. With the inherent nature of high molecular weight, raw coal requires chemical conversion to make full use of it [6–8]. The conversion of coal to clean liquid fuel products through direct coal liquefaction under high temperature and high pressure hydrogenation is ideal for producing petroleum substitutes [9]. In this process, organic soluble heavy by-products mainly including asphaltene (toluene soluble) and preasphaltene (toluene insoluble and tetrahydrofuran soluble) are generated [10, 11]. How to convert these heavy products into high valued materials is of great significance to improve coal's comprehensive utilization.

Fluorescent carbon dots (CDs), as a new class of luminescent nanomaterials, have shown potential applications in photoelectricity, catalysis, and sensor, owing to their high quantum yields, tunable photoluminescence, and convenient preparation [12–18]. To date, the synthesis of CDs can be divided into carbonization of small organic molecules (“bottom-

up” strategy) and cutting of large-sized carbon materials (“top-down” strategy) [19, 20]. Typically, chemical oxidation [21], laser ablation [22], arc discharge [23], or hydrothermal synthesis [24] were commonly employed. For instance, Wang et al. [25] used liquid fuels as raw material to prepare CDs via chemical oxidation approach for Cu^{2+} ions sensing in rat brain microdialysate. Yu et al. [26] reported employing toluene as carbon precursor to produce CDs by unfocused laser irradiation approach. However, these methods involved using highly oxidizing reagents (e.g., HNO_3 and H_2SO_4) or complex equipment. Therefore, exploring green synthetic strategy with cheap raw materials for luminescent CDs is still desirable.

The 2,4,6-trinitrophenol (TNP), as one of nitroaromatic explosives, had been used extensively in the military industrial during the First World War, because it possesses far more potent explosive violent than of 2,4,6-trinitrotoluene (TNT) [27, 28]. Currently, TNP has been widely used to fabricate dyes, pigments, pesticides, and pharmaceuticals [29, 30]. TNP easily causes water and soil pollution, which is inevitably discharged into the human living environment [31]. Furthermore, TNP is a potent allergen and irritant, long-term exposure of which may cause several health problems such as anemia, abnormal liver functions, and skin irritation [32]. Additionally, TNP may convert into its by-products, which have more additional mutagenic activity than TNP itself

[33]. Therefore, urgent needs led us to develop a rapid, sensitive and selective detection method for TNP among various nitroaromatic explosives for monitoring environmental pollution and protecting human health.

Herein, we developed a micelle-based fluorescent nanoprobe to detect TNP in water samples. The nanoprobe was made of asphaltene-based CDs and nonionic type polymeric micelles. Asphaltene-based CDs were synthesized by a microwave radiation method using asphaltene as raw material. This synthesis process is friendly and no waste products are generated. The asphaltene-based CDs were encapsulated in micelle formed by self-assembly of Pluronic F-127, which was the representative nonionic poly(ethylene oxide)-poly(propylene oxide)-poly(ethylene oxide) tri-block copolymers. The micellar probe exhibited excellent fluorescent emission at 390 nm under 320 nm excitation. Additionally, the fluorescent emission of micellar probe can be effectively quenched by TNP with energy and electron transfer mechanism. Thus, the developed probe exhibits high sensitivity and selectivity toward TNP.

Experimental section

Chemical and materials

Coal liquefaction residue is derived from the PDU pilot-plant in Shanghai Institute of Shenhua Co., Ltd. Pluronic® F-127 (F-127) was purchased from Sigma-Aldrich. 2,4,6-trinitrophenol (TNP), 2,4,6-trinitrotoluene (TNT), 2,4-dinitrotoluene (DNT), p-nitrotoluene (NT), and p-nitrophenol (NP) were purchased from Shandong West Asia Chemical Industry Co., Ltd. Phenol, acetonitrile, 1-octadecene (ODE), cyclohexane, n-hexane, toluene, and dichloromethane (DCM) were from Shanghai Titan Technology Co., Ltd.,

Extraction of asphaltene from coal liquefaction residue

The asphaltene used in this study was obtained by solvent extraction [34]. Briefly, coal liquefaction residue was wrapped with filter paper and placed in a Soxhlet extractor, which was continuously extracted with n-hexane to remove heavy oil without distillate that was from coal after high temperature and high

pressure hydrogenation. Then, the n-hexane insoluble fraction was further extracted with toluene, and the extraction solvent was treated with rotary evaporation. The residual solid from rotary evaporation were dried under vacuum at 80 °C for 24 h and the asphaltene was obtained (asphaltene is soluble in toluene and insoluble in n-hexane).

Synthesis of asphaltene-based CDs

The preparation of asphaltene-based CDs employed microwave-assisted synthesis method. In brief, asphaltene was milled firstly using a planetary ball mill for 2 h to obtain ultrafine powder. Then, 20 mg of asphaltene powder was added into 100 mL of ultrapure water in a 250 mL four-necked flask. The mixture was heated to 100 °C in the multifunctional microwave synthesizer (Sineo, UWave-2000, 2450 MHz, 600 W) and kept for 6 h under vigorous stirring. After cooling down to room temperature, the asphaltene-based CDs dispersion was obtained by removing unreacted asphaltene via centrifugation (10000 rpm for 10 min).

Probe assembling and fluorescence detection of TNP

Firstly, 0.4 g of surfactant F-127 was added into 15 mL of CDs dispersion under magnetic stirring overnight at room temperature to form the micellar nanoprobe. Then, a series of different concentrations of TNP was added into 1 mL of nanoprobe dispersion. The emission spectra were measured under the excitation wavelength of 320 nm after mixed evenly. The selectivity of nanoprobe was evaluated by adding various explosives instead of TNP in a similar way, including TNT, DNT, NP, NT, and phenol.

Results and discussion

Green synthesis of asphaltene-based CDs

The asphaltene for CDs preparation was obtained from direct coal liquefaction as a kind of heavy by-product. Oxidation and carbonization were key processes to transform the carbon-rich asphaltene to CDs. Traditional methods employed oxidizing reagents, such as HNO₃ and H₂SO₄, raising the pollution of wastewater [35]. In this work, microwave-

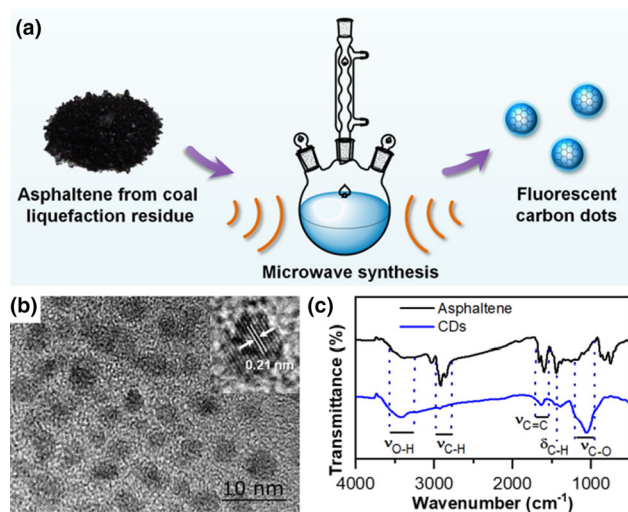


Figure 1 **a** Schematic representation of the synthesis process for the asphaltene-based CDs. **b** TEM image of the CDs. Inset: high-resolution TEM image. **c** FT-IR spectra of the asphaltene and CDs.

assisted synthesis was utilized to carbonize asphaltene/water mixture under air condition, while the molecule oxygen could participate in asphaltene oxidation (Fig. 1a). After microwave irradiation for 6 h, the generated CDs were dispersed in water (Fig. S1), which can be easily separated by removing large-sized asphaltene.

The morphology of CDs was characterized by TEM firstly. The image in Fig. 1b showed that the CDs were quasi-spherical in shape and the average size was 3.2 nm (Fig. S2). High-resolution TEM image (inset of Fig. 1b) indicated the lattice spacing of about 0.21 nm, which could be attributed to the (100) plane of graphitic carbon [36]. UV-vis absorption spectrum of CDs confirmed the $\pi-\pi^*$ transition of the aromatic carbon core (Fig. S3). The FT-IR spectra confirmed the structure change under the microwave-assisted preparation process. Compared with asphaltene, the stretching vibration (2850 and 2918 cm^{-1}) and the bending vibration (1425 cm^{-1}) of the C-H in the CDs were significantly attenuated, while the vibration of the O-H (3300–3500 cm^{-1}) and C-O (1055 cm^{-1}) were enhanced. The increase of oxygen-containing functional groups indicated the oxidation process during microwave irradiation.

Moreover, the XPS measurement (Fig. 2) was taken further to confirm the chemical composition of the asphaltene-based CDs. The XPS survey spectrum showed that CDs mainly contained C (56.49%) and O (42.25%) elements, while a handful of N (1.18%) and

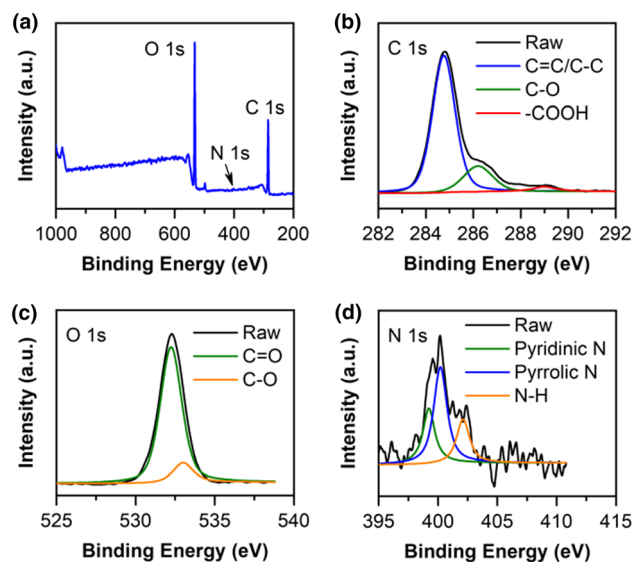


Figure 2 **a** XPS full survey of asphaltene-based CDs, and the high-resolution spectra of **b** C 1 s, **c** O 1 s, and **d** N 1 s.

S (0.07%) were existed (Table S1). The high-resolution C 1 s spectrum showed C-C/C=C (284.7 eV), C-O (286.2 eV), and -COOH (289.1 eV). The O 1 s signal could be divided into two peaks, which were attributed to C=O (532.2 eV) and C-O (533.0 eV). The weak N 1 s peak was deconvoluted into three components: pyridinic N (399.2 eV), pyrrolic N (400.2 eV), and N-H (402.1 eV) [37]. Taken structure characterizations together, the asphaltene-based CDs prepared by microwave irradiation possess a high carbonization degree and a small amount of oxygen-containing chemical groups on the surface.

The fluorescent properties of CDs

The synthesized CDs exhibited desired fluorescence properties in water dispersion. Figure 3a depicts a blue emission band of asphaltene-based CDs with maximum emission wavelength at 390 nm under UV light excitation. The emission intensity of CDs reached the maximum when the excitation wavelength was 270 nm. Simultaneously, the variation of excitation wavelength did not change the position of blue emission peak (Fig. S4). Very strikingly, the developed CDs exhibited more hydrophobic phenomenon due to the existence of crystalline carbon. As shown in Fig. 3b, the CDs in water were extracted with organic solvent (dichloromethane or 1-octadecene), and apparent blue fluorescence was observed in the organic phase. The amount of -OH

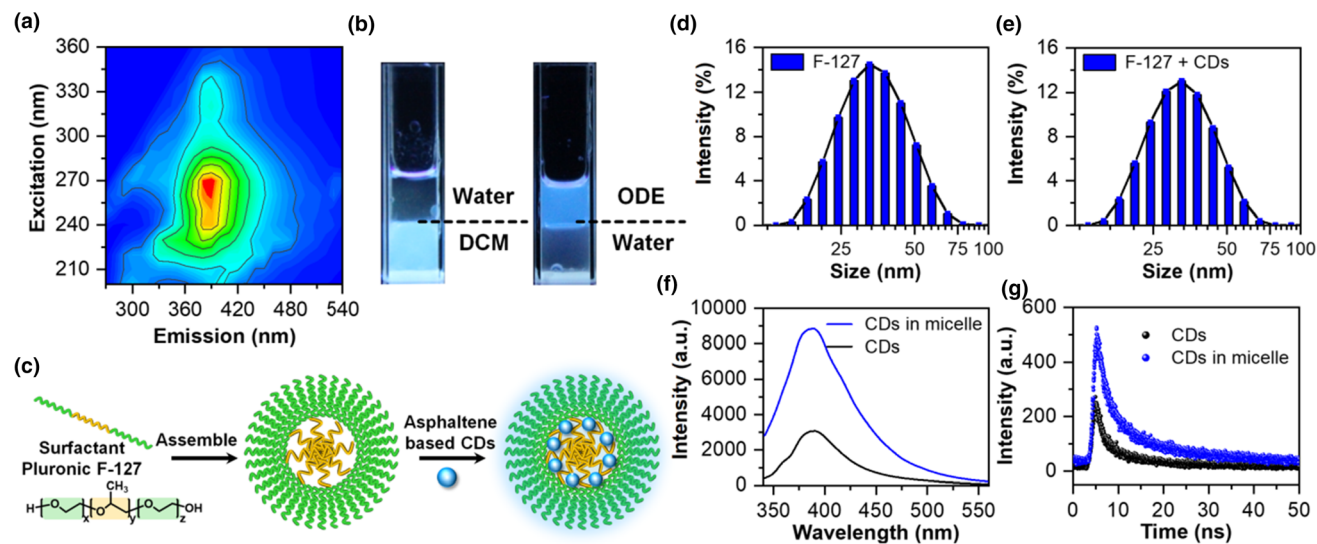


Figure 3 **a** 3D fluorescence image of asphaltene-based CDs dispersion (0.1 mg/mL). **b** Optical photographs of the mixture of asphaltene-based CDs dispersion with dichloromethane (DCM, left) and 1-octadecene (ODE, right) under ultraviolet light. **c** Schematic illustration of the process for self-assembly of F-127 into micelle with asphaltene-based CDs. **d** Size distribution

of F-127 micelle from DLS. **e** Size distribution of F-127 micelle with asphaltene-based CDs from DLS. **f** Fluorescent emission of CDs dispersion (0.1 mg/mL) with and without F-127 micelle. **g** Fluorescent decay curves of CDs dispersion (0.1 mg/mL) with and without F-127 micelle.

and $-\text{COOH}$ groups of CDs was not enough to support the highly hydrophilic feature. According to this peculiarity, we designed a micelle-enhanced strategy to improve the water dispersibility of CDs (Fig. 3c). The nonionic block copolymer F-127 was used to form nanomicelle with hydrophilic surface and hydrophobic core [38, 39]. The size of nanomicelle measured by dynamic light scattering (DLS) was about 32.75 nm (Fig. 3d). The asphaltene-based CDs could enter the core of nanomicelle after vigorous stirring owing to the hydrophobic property and small size. The size of formed CDs-micelle was 32.65 nm (Fig. 3e), which indicated that the loading of CDs caused negligible effect on the size of the micelles. More importantly, the emission intensity increased significantly by the protection of nanomicelle. Fluorescent emission spectra in Fig. 3f showed that the emission intensity of CDs in nanomicelle increased by 2.89 times without shifting of emission. Meanwhile, the fluorescent lifetime of CDs increased from 8.14 to 10.56 ns due to the protective effect of micelles (Fig. 3g and Table S2). The CDs-micelle dispersion also exhibited high stability. After one month of storage at room temperature, negligible precipitation or fluorescence decline was observed for the nanomicelle protected CDs (Fig. S5).

Fluorescence detection of TNP

Thanks to the excellent dispersibility and outstanding fluorescent emission, the CDs in nanomicelle can be employed as a nanoprobe for fluorometry. Because of the carbon conjugate structure and hydrophobic characteristics of asphaltene-based CDs, we tested the sensitivity of nanoprobe to TNP. As shown in Fig. 4a, the emission of the micellar probe at 390 nm was significantly quenched by TNP, and the fluorescent intensity was reduced by 76% after the addition of TNP with 48 μM . The result demonstrated that the asphaltene-based CDs micellar probe

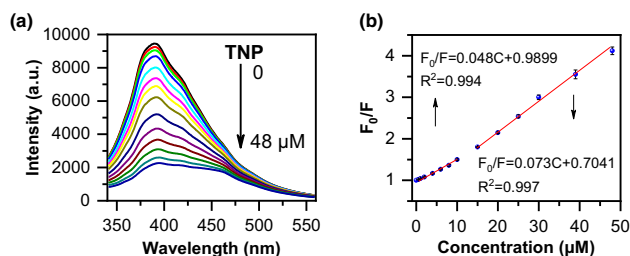


Figure 4 **a** The emission spectra of asphaltene-based CDs in F-127 micelle (excitation: 320 nm) with different amount of TNP. **b** The linear relationship of fluorescence quenching F_0/F versus the concentration of TNP.

had an extremely sensitive response to TNP. By plotting the F_0/F versus the concentrations of TNP (F_0 and F represented the fluorescent intensities at 390 nm without and with TNP, respectively), the linear range can be obtained ranging from 0.5 to 10 μM and 15 to 48 μM , respectively (Fig. 4b). The limit of detection (LOD) was estimated to be 0.21 μM . By comparison with the reported literatures, it is clear that the developed method exhibits superiority in terms of sensitivity for TNP determination (Table S3), which guarantees the detection of TNP in water samples.

Mechanism study

In order to understand the origin of the high sensitivity of the fluorescent CDs-micelle dispersion toward TNP, the intrinsic mechanism of quenching was further investigated. As shown in Fig. 5a, there is a spectral overlap between the absorption of TNP and the emission of asphaltene-based CDs, which permits the energy transfer from the excited state of CDs to the ground state of TNP, resulting in the fluorescence quenching of CDs [30]. Meanwhile, the introduction of TNP shortened the lifetime of excited state of CDs (Fig. 5b and Table S2), the fluorescent lifetime of CDs in micelle was 10.56 ns, but it reduced to 9.19 ns when 30 μM of TNP was added. This result further proved the mechanism of energy transfer. Moreover, spectral overlap between the absorption of TNP and the excitation/emission of CDs could lead to the quenching by inner filter effect at high concentration of TNP.

The selectivity experiment revealed a coexisting quenching pathway. We compared the fluorescence quenching with structure similar aromatic nitro-compounds, including p-nitrophenol (NP), phenol, 2,4-dinitrotoluene (DNT), p-nitrotoluene (NT), and

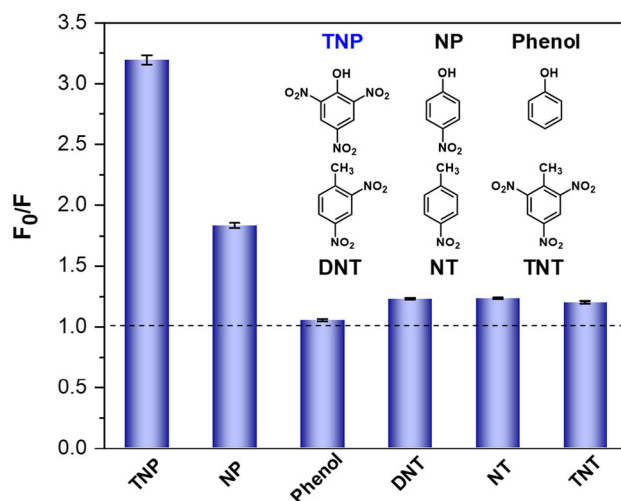
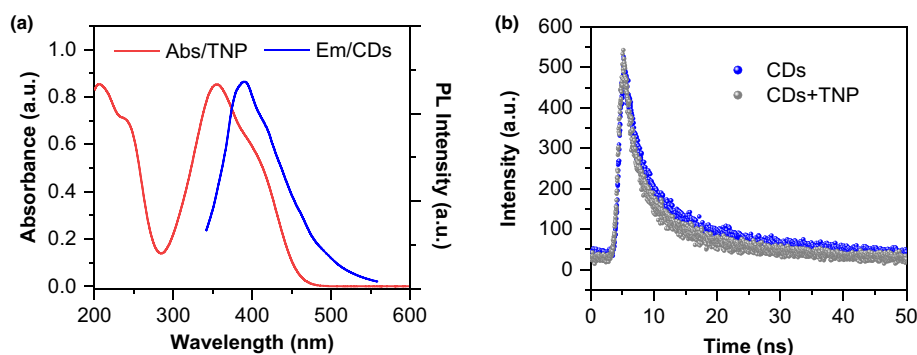


Figure 6 The selectivity of micellar nanoprobe toward structure similar analytes. The concentration of all of the analytes is 30 μM . F_0 and F represented the fluorescent intensities at 390 nm without and with the analyte, respectively.

2,4,6-trinitrotoluene (TNT). As shown in Fig. 6, quenching efficiency for TNP was much higher than other nitro-compounds and phenol. However, these compounds can also cause small amounts of fluorescence quenching. The UV-vis spectra showed that none of these compounds had significant absorption at the emission band of asphaltene-based CDs except NP (Fig. S6). This suggests that there are still other forms of quenching mechanism besides energy transfer. Due to the presence of nitro group, these compounds exhibit strong electron-deficient properties. Thus, the electron transfer from asphaltene-based CDs to the acceptor of aromatic nitro-compound occurred [40]. As shown in Fig. 7, the quenching efficiency was evaluated with the Stern-Volmer equation: $(F_0/F) = 1 + K_{sv}[TNP]$. The K_{sv} value for TNP was calculated to be $6.778 \times 10^4 \text{ M}^{-1}$, indicating the high quenching efficiency. NP resulted

Figure 5 **a** The absorption spectrum of TNP and emission spectrum of asphaltene-based CDs in F-127 micelle. **b** Fluorescent decay curves of CDs in F-127 micelle without and with 30 μM of TNP.



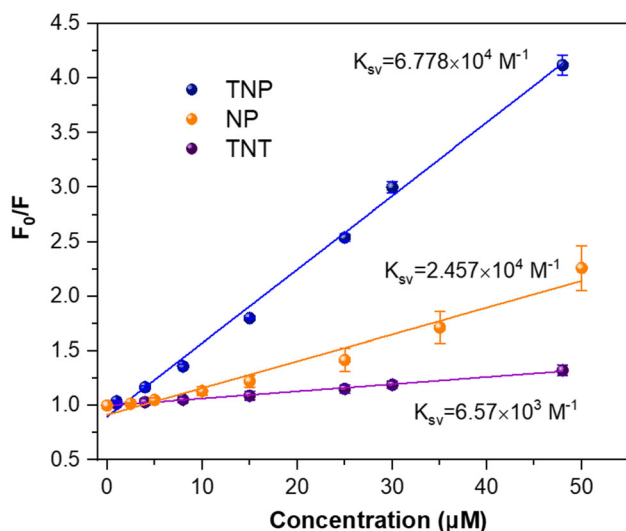


Figure 7 Stern–Volmer plot of the micellar probe in the presence of TNP, NP, and TNT, respectively.

in the K_{sv} of $2.457 \times 10^4 \text{ M}^{-1}$, due to the energy transfer and electron transfer mechanisms. Since only electron transfer quenching exists, the K_{sv} value for TNT is $6.57 \times 10^3 \text{ M}^{-1}$, which is an order of magnitude lower than that of TNP. The above results indicated that the quenching of asphaltene-based CDs by TNP was induced with energy transfer and electron transfer, providing outstanding selectivity to TNP.

Lake water analysis

To explore actual applications of the developed asphaltene-based CDs probe, we have utilized it to quantitatively determine TNP in lake water samples from our campus. The various concentrations of TNP were added into the resultant water sample and analyzed with the proposed method. The determination results are shown in Table 1. It was evident that spiked recoveries were in the range of 98.2–105.6%, and the RSD was lower than 1.84%. As a consequence, the developed fluorescent probe was effective to TNP and the coexisting substances in lake

Table 1 Recovery test of proposed method for TNP in lake water

Sample	Spiked (μM)	Found (μM)	Recovery (%)	RSD (%)
1	5	5.19	103.8	1.84
2	10	10.56	105.6	1.57
3	15	14.73	98.2	1.59

water caused negligible interference. This result indicated that the present method has great potential for determination of TNP in real samples.

Conclusions

In conclusion, a new type of fluorescent probe was developed using asphaltene-based CDs as a fluorophore. Conversion of asphaltene into functional CDs with fluorescent properties improved the comprehensive utilization of coal. The proposed probe exhibited superior sensitivity to aromatic nitro-compound of TNP. Mechanism studies recovered that energy transfer and electron transfer were the main cause of fluorescence quenching. We hope these results would offer a novel idea to design CDs-based sensor with resource-saving, sensitivity, and convenience.

Acknowledgements

This work was supported by the National Natural Science Foundation of China (22106005), the Natural Science Foundation of Anhui Province (1908085MB41), and Anhui Province Key Laboratory of Coal Clean Conversion and High Valued Utilization (CHV21-05).

Author's contribution

ML contributed to investigation, visualization, and writing—original draft. XL contributed to methodology and formal analysis. YZ contributed to formal analysis and validation. YZ contributed to visualization. TL contributed to formal analysis. ZH contributed to validation. CZ contributed to conceptualization, investigation, and writing—original draft. KZ contributed to supervision and writing—original draft.

Declarations

Conflict of interest The authors declare that they have no known competing financial interests or personal relationships that could have appeared to influence the work reported in this paper.

Supplementary Information: The online version contains supplementary material available at <http://doi.org/10.1007/s10853-022-08076-w>.

References

- [1] He M, Sun Y, Han B (2013) Green carbon science: Scientific basis for integrating carbon resource processing, utilization, and recycling. *Angew Chem Int Ed* 52:9620–9633
- [2] Zhao Y, Cui Z, Wu L, Gao W (2019) The green behavioral effect of clean coal technology on China's power generation industry. *Sci Total Environ* 675:286–294
- [3] Xu XY, Liu Y, Zhang F, Di W, Zhang YL (2017) Clean coal technologies in China based on methanol platform. *Catal Today* 298:61–68
- [4] Dmitrienko MA, Nyashina GS, Strizhak PA (2018) Major gas emissions from combustion of slurry fuels based on coal, coal waste, and coal derivatives. *J Cleaner Prod* 177:284–301
- [5] Yao ZT, Ji XS, Sarker PK, Tang JH, Ge LQ, Xia MS, Xi YQ (2015) A comprehensive review on the applications of coal fly ash. *Earth-Sci Rev* 141:105–121
- [6] Mochida I, Okuma O, Yoon SH (2014) Chemicals from direct coal liquefaction. *Chem Rev* 114:1637–1672
- [7] Wang Z, Wang Q, Hu R, Pan C, Wang X, Ren S, Lei Z, Kang S, Yan J, Shui H (2019) Effect of thermal extraction on hydro-liquefaction property of residual coal. *Fuel* 251:474–481
- [8] Wu H, Xiao J, Zeng X, Li X, Yang J, Zou Y, Liu S, Dong P, Zhang Y, Liu J (2019) A high performance direct carbon solid oxide fuel cell-A green pathway for brown coal utilization. *Appl Energy* 248:679–687
- [9] Vasireddy S, Morreale B, Cugini A, Song C, Spivey JJ (2011) Clean liquid fuels from direct coal liquefaction: chemistry, catalysis, technological status and challenges. *Energy Environ Sci* 4:311–345
- [10] Li X, Chi P, Guo X, Sun Q (2019) Effects of asphaltene concentration and asphaltene agglomeration on viscosity. *Fuel* 255:115825
- [11] Qin F, Guo Z, Wang J, Qu S, Zuo P, Shen W (2019) Nitrogen-doped asphaltene-based porous carbon nanosheet for carbon dioxide capture. *Appl Surf Sci* 491:607–615
- [12] Liu ML, Chen BB, Li CM, Huang CZ (2019) Carbon dots: synthesis, formation mechanism, fluorescence origin and sensing applications. *Green Chem* 21:449–471
- [13] Li M, Chen T, Gooding JJ, Liu J (2019) Review of carbon and graphene quantum dots for sensing. *ACS Sens* 4:1732–17480
- [14] Xia C, Zhu S, Feng T, Yang M, Yang B (2019) Evolution and synthesis of carbon dots: from carbon dots to carbonized polymer dots. *Adv Sci* 6:1901316
- [15] Liu Y, Li W, Wu H, Lu S (2021) Carbon dots enhance ruthenium nanoparticles for efficient hydrogen production in alkaline. *Acta Phys-Chim Sin* 37:2009082
- [16] Fan ZY, Liu ZJ, Zhang RL, Han GM, Zhang ZP (2021) Preparation of lysosome-targeting carbon dots and its application in cell imaging. *Chin J Anal Chem* 49:1208–1217
- [17] Wang Y, Li X, Zhao S, Wang B, Song X, Xiao J, Lan M (2022) Synthesis strategies, luminescence mechanisms, and biomedical applications of near-infrared fluorescent carbon dots. *Coord Chem Rev* 470:214703
- [18] Han G, Zhao J, Zhang R, Tian X, Liu Z, Wang A, Liu R, Liu B, Han MY, Gao X, Zhang Z (2019) Membrane-penetrating carbon quantum dots for imaging nucleic acid structures in live organisms. *Angew Chem Int Ed* 58:7087–7091
- [19] Li Z, Wang L, Li Y, Feng Y, Feng W (2019) Frontiers in carbon dots: design, properties and applications. *Mater Chem Front* 3:2571–2601
- [20] Gao J, Zhu M, Huang H, Liu Y, Kang Z (2017) Advances, challenges and promises of carbon dots. *Inorg Chem Front* 4:1963–1986
- [21] Hu C, Yu C, Li M, Wang X, Yang J, Zhao Z, Eychmüller A, Sun Y, Qiu J (2014) Chemically tailoring coal to fluorescent carbon dots with tuned size and their capacity for Cu(II) detection. *Small* 10:4926–4933
- [22] Calabro RL, Yang DS, Kim DY (2018) Liquid-phase laser ablation synthesis of graphene quantum dots from carbon nano-onions: Comparison with chemical oxidation. *J Colloid Interface Sci* 527:132–140
- [23] Xu X, Ray R, Gu Y, Ploehn HJ, Gearheart L, Raker K, Scrivens WA (2004) Electrophoretic analysis and purification of fluorescent single-walled carbon nanotube fragments. *J Am Chem Soc* 126:12736–12737
- [24] Gao Y, Zhang H, Shuang S, Dong C (2020) Visible-light-excited ultralong-lifetime room temperature phosphorescence based on nitrogen-doped carbon dots for double anticounterfeiting. *Adv Optical Mater* 8:1901557
- [25] Wang C, Pan C, Wei X, Yang F, Wu W, Mao L (2020) Emissive carbon dots derived from natural liquid fuels and its biological sensing for copper ions. *Talanta* 208:120375
- [26] Yu H, Li X, Zeng X, Lu Y (2016) Preparation of carbon dots by non-focusing pulsed laser irradiation in toluene. *Chem Commun* 52:819–822
- [27] Chen X, Sun C, Liu Y, Yu L, Zhang K, Asiri AM, Marwanic HM, Tand H, Aia Y, Wanga X, Wang S (2020) All-inorganic perovskite quantum dots CsPbX₃ (Br/I) for highly sensitive

- and selective detection of explosive picric acid. *Chem Eng J* 379:122360
- [28] Bauri K, Saha B, Mahanti J, De P (2017) A nonconjugated macromolecular luminogen for speedy, selective and sensitive detection of picric acid in water. *Polym Chem* 8:7180–7187
- [29] Kathiravan A, Gowri A, Khamrang T, Kumar MD, Dhenadhayalan N, Lin KC, Velusamy M, Jaccob M (2019) Pyrene-based chemosensor for picric acid fundamentals to smartphone device design. *Anal Chem* 91:13244–13250
- [30] Wang B, Mu Y, Zhang C, Li J (2017) Blue photoluminescent carbon nanodots prepared from zeolite as efficient sensors for picric acid detection. *Sens Actuators B* 253:911–917
- [31] Parvathy PA, Dheepika R, Abhijnakrishna R, Imran PKM, Nagarajan S (2020) Fluorescence quenching of triarylamine functionalized phenanthrolinebased probe for detection of picric acid. *J Photochem Photobiol A* 401:112780
- [32] Maity S, Shyamal M, Das D, Mazumdar P, Sahoo GP, Misra A (2017) Aggregation induced emission enhancement from antipyrene-based schiff base and its selective sensing towards picric acid. *Sens Actuators B* 248:223–233
- [33] Wollin K, Dieter HH (2005) Toxicological guidelines for monocyclic nitro-, amino- and aminonitroaromatics, nitramines, and nitrate esters in drinking water. *Arch Environ Contam Toxicol* 49:18–26
- [34] Wargadalam VJ, Norinaga K, Iino M (2002) Size and shape of a coal asphaltene studied by viscosity and diffusion coefficient measurements. *Fuel* 81:1403–1407
- [35] Feng N, Li H, Hao J (2021) Toward the neutralization of carbon dots prepared by mixed acid reflux. *Acta Phys Chim Sin* 37:2005004
- [36] Jiang K, Hu S, Wang Y, Li Z, Lin H (2020) Photo-stimulated polychromatic room temperature phosphorescence of carbon dots. *Small* 16:2001909
- [37] Wu M, Wang Y, Wu W, Hu C, Wang X, Zheng J, Li Z, Jiang B, Qiu J (2014) Preparation of functionalized water-soluble photoluminescent carbon quantum dots from petroleum coke. *Carbon* 78:480–489
- [38] Zhou T, Zhu J, Gong L, Nong L, Liu J (2019) Amphiphilic block copolymer-guided in situ fabrication of stable and highly controlled luminescent copper nanoassemblies. *J Am Chem Soc* 141:2852–2856
- [39] Khalin I, Heimburger D, Melnychuk N, Collot M, Groschup B, Hellal F, Reisch A, Plesnila N, Klymchenko AS (2020) Ultrabright fluorescent polymeric nanoparticles with a stealth pluronic shell for live tracking in the mouse brain. *ACS Nano* 14:9755–9770
- [40] Sun X, He J, Meng Y, Zhang L, Zhang S, Ma X, Dey S, Zhao J, Lei Y (2016) Microwave-assisted ultrafast and facile synthesis of fluorescent carbon nanoparticles from a single precursor: preparation, characterization and their application for the highly selective detection of explosive picric acid. *J Mater Chem A* 4:4161–4171

Publisher's Note Springer Nature remains neutral with regard to jurisdictional claims in published maps and institutional affiliations.

Springer Nature or its licensor (e.g. a society or other partner) holds exclusive rights to this article under a publishing agreement with the author(s) or other rightsholder(s); author self-archiving of the accepted manuscript version of this article is solely governed by the terms of such publishing agreement and applicable law.